Published by :
http://www.ijert.org

International Journal of Engineering Research & Technology (IJERT)
ISSN: 2278-0181
Vol. 9 Issue 01, January-2020

Structural, Dielectric and Electrical Properties of Lead-free$Na_{0.5}Bi_{0.5}Ti_{0.9}Zr_{0.1}O_3$ceramics

D. Panda
PXE, DRDO, Chandipur,
Balasore, Odisha, India

P. S. Sahoo
Department of Physics,
North Orissa University, Baripada, Odisha, India

B. B. Mohanty
Department of Physics, Betnoti College Betnoti,
Mayurbhanj, Orissa, India

R. N. P. Choudhary
Department of Physics ITER,
Bhubaneswar, Odisha, India

***Abstract*:- Ceramic samples of Zirconium substituted Sodium Bismuth Barium Titanate of composition $Na_{0.5}Bi_{0.5}Ti_{0.9}Zr_{0.1}O_3$ a polycrystalline orthorhombic compound have been synthesized by conventional solid state reaction method at high temperature (i.e., at 900˚C). The impact of Zr (0·1) on the structural and microstructural properties of $Na_{0.5}Bi_{0.5}Ti_{0.9}Zr_{0.1}O_3$ was explored by XRD and SEM. The room temperature X-ray diffraction study guaranteed the advancement of single-stage compound with orthorhombic structure. The dielectric examination of $Na_{0.5}Bi_{0.5}Ti_{0.9}Zr_{0.1}O_3$ explored over an expansive frequency extend ($10^3 - 10^6$ Hz) at different temperatures (100˚C - 500˚C) showed that the dielectric properties of the material are reliant on both frequency and temperature. Dielectric study uncovers that the ferro to paraelectric stage change of the studied compound is a temperature of 300˚C. The idea of the variety of conductivity and estimation of activation energy in various regions, determined from the temperature reliance of ac conductivity recommend that the conduction process is of blended sort (for example , ionic–polaronic and space charge produced from the oxygen ion vacancies). AC impedance plots as a function of frequency at various temperatures were utilized to examine the electrical conduct of the sample, PTCR properties is seen in low temperature (≤ 200ºC) locale and above which demonstrated the negative temperature coefficient of resistance character. Complex impedance investigation focused on the relaxation phenomenon is poly disperse and non-Debye type in nature.**

Subject Areas:- Condensed State Physics

Keyword:- Ceramics, Perovskite Structure, Solid-State Reaction, X-Ray Diffraction, dielectric, impedance, diffuse phase transitions.

1. INTRODUCTION

Since the disclosure of barium titanate, BaTiO3, in polycrystalline structure, it has been comprehensively used in various electronic portions, for instance, multilayer capacitor (MLCs), positive temperature coefficients of resistivity (PTCR) thermistor, piezoelectric device, optoelectronic fragments and semiconductors (Morrison et al 2001; Weber et al 2001; Mahajan et al 2009). For MLCs applications, dielectric materials ought to be electrically ensuring (>1010 Ω cm and show high permittivity regards (> 1000) at room temperature (Morrison et al 2001). Significant properties for business contraption applications have been by and large observed at first in poisonous perovskite blends, for instance, PMN–PT, PNN–PZT, PLZT and PZT (Park and Shrout 1997; Fu and Cohen 2000; Mahajan et al 2009). These pieces have an obvious drawback of flightiness and hurtfulness of 'lead'. Producers are by and by being avoided using materials especially those containing lead. Along these lines, starting late, ask about undertakings have been facilitated more towards the improvement of biological pleasant 'without lead' creations. Reprisal the previously mentioned, the ferroelectric oxides of perovskite assistant family have fundamentally been tried for their accommodating dielectric [5], electro-optic [6], nonlinear optic [7] pyroelectric [8], piezoelectric [9] properties. A perfect perovskite structure can be addressed by a general condition as ABO3 where A will be a gigantic cation (mono to trivalent) and B is a little cation (a change metal molecule). The A particles include the edges of the 3D square, which is 12 formed, while the B particles sit on the body center situations inside an oxygen octahedron, which are at the face center positions. Literature survey unveiled that a bottomless of research has been developed on perovskite type ferroelectric oxides niobates and tantalates [11] [12] [13]. We couldn't find any, in any case, no work is executed on the assistant, dielectric and electrical properties of flow compound. Looking to the centrality of the material, we have consolidated and examined the auxiliary and dielectric properties of another compound having the invention condition $Na_{0.5}Bi_{0.5}Ti_{0.9}Zr_{0.1}O_3$.

2. EXPERIMENTAL PROCEDURE

2.1 Material preparation

The stoichiometric ratio of starting chemicals NaCO3 (>99·9%), Bi2O3 (>99·9%), TiO2 (>99·9%) and ZrO2 (>99·9%) were weighed for the composition $Na_{0.5}Bi_{0.5}Ti_{0.9}Zr_{0.1}O_3$ (x = 0.1). The gauged powders were mixed precisely by an agate mortar for around 3 h. The powders were then calcined at enhanced temperature and time (900˚C for 12 h) in cooled. The calcined powder along these lines acquired was mixed with PVA (poly vinyl liquor) cover, crushed and were palletized ensuingly (around 10 mm in width and 1 - 2 mm thickness) under

International Journal of Engineering Research & Technology (IJERT)
ISSN: 2278-0181
Vol. 9 Issue 01, January-2020

uniaxial weight of 4× 10^6 N/m2. From that point the pellets were sintered in air environment at 950˚C for 12 h. At last the pellets were covered with high virtue silver paint, and afterward warmed at 150˚C for 2 h before executing the electrical estimations.

2.2 Material characterisation

X-ray diffraction (XRD) pattern of the material acquired in a tremendous scope of Bragg edge 2θ ($20^0 \leq 2\theta \leq 80^0$)at a checking pace of 3^0/min by a X-beam diffractometer (Rigaku, Miniflex) with CuKα radiation (λ = 1.5405 A) at room temperature. The surface morphology of the pellet test of the material was recorded with a high-goals scanning electron microscope (SEM: JOEL-JSM model: 5800F). The dielectric characterisation of the example was arraigned in the temperature scope of 32˚C - 5000˚C and frequency range of 1 kHz to 1 MHz, utilizing a PC controlled Hioki HiTester LCR meter.

3. RESULTS AND DISCUSSION

3.1. Structural and Microstructural Analysis

Figure 1 and 2 shows the XRD pattern of the sample. Ordering of the considerable number of peaks of the sample were finished taking their 2θ values by a PC program package,"POWDMULT" [14] in distinct crystal system and cell arrangement and are followed to be sharp and solo, which The peaks are discrete from those of ingredients guaranteeing the advancement of new single-stage compound. Based on the best understanding (in light of least-squares refinement) between investigated (obs) and figured (cal) inter planer separation d (i.e., Σ (dobs − dcal) = least), an orthorhombic unit cell was chosen with cross section parameters: a = 23.6720 (29) Å, b =8.5031 (29) Å, c = 7.5427 (29) Å (evaluated standard deviation in enclosures) which are consistence with the announced ones [15].

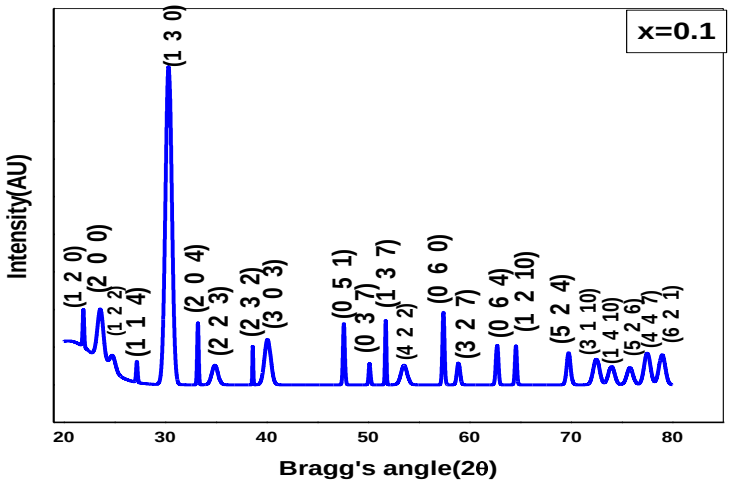

Figure 1. Room temperature XRD pattern of $Na_{0.5}Bi_{0.5}Ti_{0.9}Zr_{0.1}O_3$compound.

The soundly normal scattered crystallite size (D) of the compound was figured to be ~ 15 nm utilizing Scherrer's condition; D = 0.89λ/(β1/2cosθhkl), where λ = 1.5405 A and β1/2 = peak width of the reflection at half maxima [16]. The commitments of strain, instrumental mistake and other obscure impacts in the peak widening have not been taken into board during the crystallite size list. The room temperature SEM micrograph (Figure 2 (left) of the NBTZ compound, affirmed homogenously and non-uniform distribution of the grains over the whole surface of the sample. The grain size assessed from the histogram Figure 2 (right) is followed to be of 6.9 µm. True to form, the grain size of the sample acquired here is immense in contrast with the crystallite size identified from Scherrer's condition. Subsequently, a performance grain has enormous number of crystallites [17].

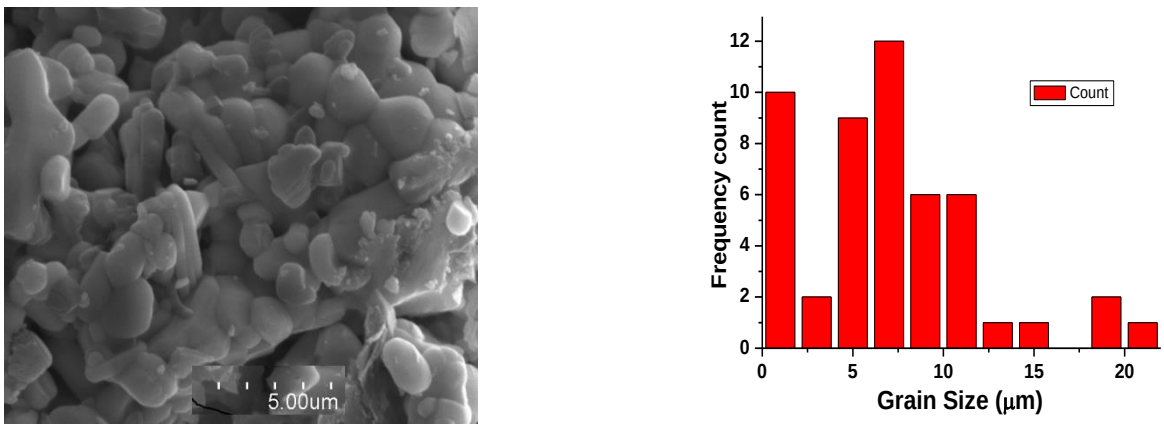

Fig:2 SEM micrographs and histogram (left) and and histogram (right) of $Na_{0.5}Bi_{0.5}Ti_{0.9}Zr_{0.1}O_3$ compound.

International Journal of Engineering Research & Technology (IJERT)
ISSN: 2278-0181
Vol. 9 Issue 01, January-2020

3.2. Dielectric Analysis

The variation of dielectric parameters (relative dielectric permittivity (ε_r) and loss tangent (tanδ) with frquency is shown in Fig.3. Both dielectric permittivity (ε_r) and loss tangent (tanδ) decline forcefully with the ascent in frequency which is a general property of dielectric materials [4,5].The estimation of dielectric constant decreases at higher frequencies, and inevitably arrives at a steady worth that might be expected to the more slow development/jumping of electrons in dielectric materials [22]. The electron jumping at high frequencies can't follow the changing electric field thus they need to travel through grain and grain boundaries. Since the grain boundaries have high obstruction it causes space charge polarization as the electrons pileup there which expands dielectric constant at a lower frequency. At higher frequency dielectric constant decays as the collection of charges at grain boundaries diminishes. The Maxwell-Wagner and Koop's phenomenological models clarify such kind of dielectric conduct (i.e., in the area of lower frequency the dielectric constant decreases rapidly while at higher frequency locale it decays gradually) [23]. In light of these models, the structure of the dielectric material is partitioned into two layers (i.e., the exceptionally leading grains viable at high frequency and ineffectively directing grain boundaries viable at lower frequencies). The tangent loss (tanδ) changes along these lines, as in that of (ε_r) with frequency. The tanδ is normally higher in the lower frequency locale because of higher obstruction of grain boundaries for which more energy is required for the development of electrons. In the higher locale of frequency, the opposition is low which demonstrates lower estimation of tanδ This may be due to the dielectric relaxation phenomena occurring in the compound [24].

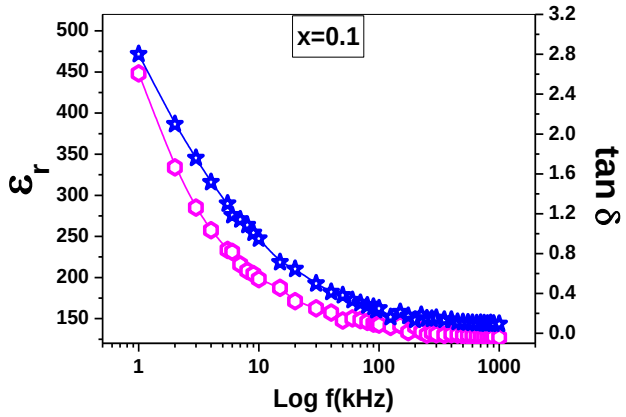

Fig.3. ε_r ~ logf & tanδ ~ log f graphs of $Na_{0.5}Bi_{0.5}Ti_{0.9}Zr_{0.1}O_3$ at room temperatures

The temperature assortment of relative dielectric constant (εr) at some picked frequencies of compound is shown Figure 4. The plot decidedly settled the ferro to paraelectric arrange progress at 268˚C. The estimation of εr is little at low temperatures which increases with rise in temperature. The dielectric constant (εr) at frequencies 10, 50, 100, 500 and 1000 kHz are viewed as 352, 225, 198, 170 and 162 individually at the transition temperature. The assortment of tanδ seeks after a comparative pattern as that of εr . The extension in the estimation of tanδ may be relied upon to (i) improvement in the conductivity and (ii) decline in the responsibility of ferroelectric domain wall [18].

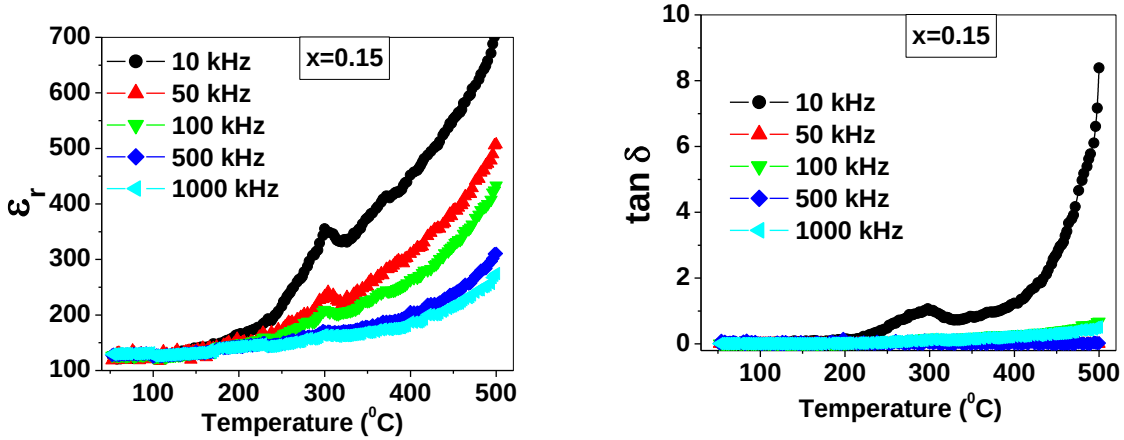

Figure 4. Variation of εr and tanδ (right) with temperature of $Na_{0.5}Bi_{0.5}Ti_{0.9}Zr_{0.1}O_3$ at some selected frequencies.

International Journal of Engineering Research & Technology (IJERT)
ISSN: 2278-0181
Vol. 9 Issue 01, January-2020

3.3. Ac Conductivity Analysis

The ac electrical conductivity (σ_{ac}) is resolved using the dielectric data and an exact association $\sigma_{ac} = \omega \in_r \in_0 \tan\delta$, where $\in_0$ = permittivity of free space and ω = angular frequency. Figure 5 shows the variety of σ_{ac} as a component of temperature at frequencies 10 and 100 kHz. The idea of the variety (Figure 5) is practically straight over a wide temperature zone conforming to the Arrhenius relation: $\sigma_{ac} = \sigma_0 \exp(-E_a/k_B T)$ [19], every one of outlines is separated into two unique regions autonomously of frequency. Each partitioned locale is portrayed by various slopes indicating distinctive activation energy. The solid line of figure shows the linear fit. The activation energy determined from the slope of the curve at various temperatures has been looked at in Table 1. In light of the dielectric phase transition, variation from the norm in conductivity was watched for the whole compound at temperatures about equivalent to its Curie temperature, which might be a result of the dielectric phase transition. The estimation of σ_{ac} increments with increment in temperature demonstrating negative temperature coefficient of resistace (NTCR) behaviour. The expansion in conductivity is because of the jumping activity of the ions in view of thermally initiated electrons. At high temperature higher estimation of activation energy demonstrates that conductivity is for the development of oxygen vacancies. Activation energy is low at high frequency when contrasted with that at the low frequency (Table 1). This is on the grounds that at low frequencies the general conductivity is the consequence of jumping of charge carriers over a huge separation and at higher frequencies is limited to just closest neighboring imperfections sites [20].

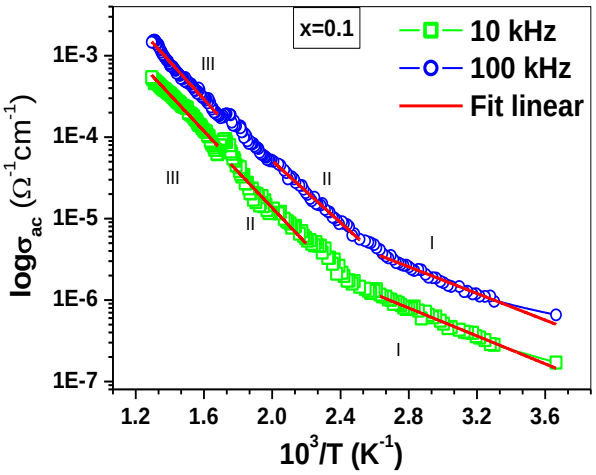

Figure 5. Variation of σ_{ac} with 1000/T of $Na_{0.5}Bi_{0.5}Ti_{0.9}Zr_{0.1}O_3$at two selected frequencies.

Table 1. Comparison of activation energy Ea (eV) of $Na_{0.5}Bi_{0.5}Ti_{0.9}Zr_{0.1}O_3$at two different frequencies in region I, II and III, calculated from σ_{ac} vs. 1/T graphs.

		Activation energy E_a (eV)		
Frequency (kHz)		Region I	Region II	Region III
10	0.1701	0.4385	0.4454	
100	0.1623	0.3752	0.4390	

3.4 Complex immittance spectroscopy

Complex impedance spectroscopy procedure is a successful and basic adaptable technique to break down the frequency subordinate response of different electrical parameters and impacts (grain, grain boundaries and electrode impact and so forth.) of the compound related to basic impedance detailing. The yield response in the contemplated sample is estimated by applying an ac signal over the sintered pellet. Fig. 6 demonstrates the frequency reliance of impedance plots at the chose temperatures. The diminishing idea of the real part of impedance (Z') with the expansion in frequency and temperature can be shown in the figure. In the high-frequency region, Z' matches with one another to accomplish a roughly consistent worth. The total converging of the curves of Z' for various temperature at high frequencies (over 100 kHz) might be because of the semiconductor properties, and arrival of space charges. The declining pattern of Z' esteem uncovers the nearness of negative temperature coefficient of resistance behaviour in the material [25].

International Journal of Engineering Research & Technology (IJERT)
ISSN: 2278-0181
Vol. 9 Issue 01, January-2020

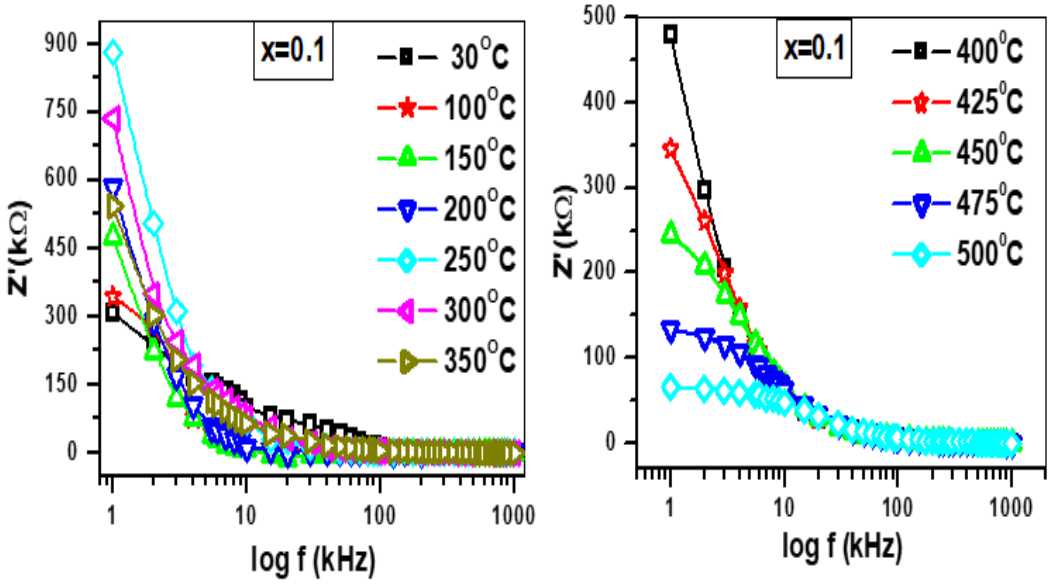

Fig 6. Z′~ log f of $Na_{0.5}Bi_{0.5}Ti_{0.9}Zr_{0.1}O_3$at various temperatures

Figure 7(a and b) and figure 8 speaks to the variety of imaginary part of impedance (Z″) and modulus as a component of frequency at various temperatures for **$Na_{0.5}Bi_{0.5}Ti_{0.9}Zr_{0.1}O_3$** ceramic. In the lower frequency side, ordinary varieties in Z″ values with temperature and frequency were watched and every one of the curves at various temperatures seem to converge in to a solitary curve in the higher frequency locale (figure 6 a and b). The decrease in Z" with increment in temperature beneath 200°C affirms PTCR behaviour of the compound or more that NTCR behaviour is watched. The moving of the Z″max in the direction of high frequency side in high temperature region is a consequence of relaxation phenomenon in the system. The reduction in resistance of grain when temperature rises is the cause of the shifting of peaks. Merging of all these curves at fusion frequency (f_f) is a symptom of the gathering of space charge in the studied compounds [21]. The low frequency area peak compares to grain boundary, while higher frequency region peak speaks to the bulk (grain) commitment. Decrement in peak height of the impedance spectra with rise in temperature is a characteristic feature very familiar in polycrystalline ceramics [22-24] which indicates temperature evolutions of relaxation processes. The estimation of resistance and capacitance for grain and grain boundary were gotten utilizing the relation $2\pi\ fmRC = 1$ from from Z″ versus log f plot and showing commitments from grain and grain boundary in the samples.

Table 2. Resistance (Rg, Rgb) and capacitance (Cg, Cgb) of grains and grain boundaries of $Na_{0.5}Bi_{0.5}Ti_{0.9}Zr_{0.1}O_3$ ceramics

Temperature (□C)	*Rg* (Ω)	*Cg* (F)	*Rgb* (Ω)	*Cgb* (F)
400	**6.842E+005**	**4.720E-011**	**7.695E+002**	**1.070E-010**
425	**3.966E+005**	**4.287E-011**	**1.758E+001**	**1.133E-010**
450	**2.631E+005**	**4.761E-011**	**5.378E+003**	**1.186E-010**
475	**1.370E+005**	**4.499E-011**	**3.595E+003**	**1.653E-010**
500	**6.624E+004**	**8.887E-020**	**5.630E+001**	**2.608E-010**

The figure 6 shows the plot of imaginary part M″ with frequency at various temperatures. The utilization of modulus spectroscopic plot is especially helpful for isolating segment with comparable resistance however extraordinary capacitance. In figure 6, peaks give off an impression of being moved towards higher frequency side with ascend in temperature. It is additionally seen that M″ peaks expand with decline in temperature. The watched temperature and frequency reliance of M″ emerges because of conveyance of relaxation time in the sample. The expanding of M" spectra must be inherently non-exponential process, as entomb relationship among diffusion of the charged species, or assorted varieties in the microstructure of the material, driving consecutively circulation of conduction of confined charged species in space and time to react electrical impact.

International Journal of Engineering Research & Technology (IJERT)
ISSN: 2278-0181
Vol. 9 Issue 01, January-2020

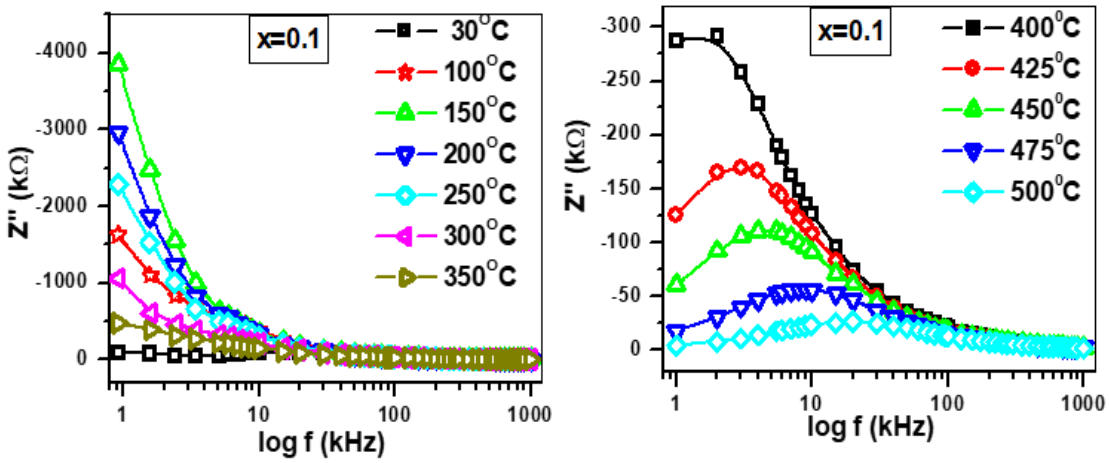

Fig 7.(a) Fig 7.(b)

Figure 7. (a) and (b): Frequency dependence of imaginary part of impedance Z'' at different temperatures for $Na_{0.5}Bi_{0.5}Ti_{0.9}Zr_{0.1}O_3$ ceramic sample.

3.5 Nyquist plot

The Nyquist graph (impedance range) shows the variety of the real part of impedance (Z') with its imaginary (Z'') .The impedance attributes of the sample demonstrate the nearness of bulk, grain boundary and electrode interfaces impacts in the material. With an ascent in temperature, the impedance curves steadily bend to frame semicircle (appeared in embedded Fig. 9) with the adjustment in their middle point to the starting point of the plot. This deviation in the pattern of the semicircular arc with variety in temperature proposes the impedance normal for the sample. In light of the investigation of the attributes of the two semicircles framed in the temperature range of 100–475°C, we can presume that the compound has both grain and grain boundary impacts in the electrical properties. The estimations of grain resistance (Rg), grain boundary resistance (Rgb), grain capacitance (Cg) and grain boundary capacitance (Cgb) are appeared in table 2.

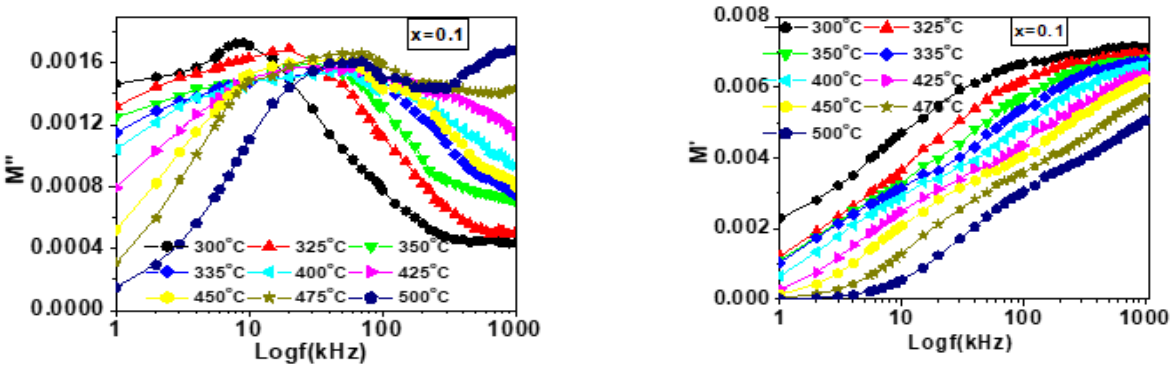

Figure 8. Frequency dependence of real M' & imaginary part of modulus M'' at different temperatures for $Na_{0.5}Bi_{0.5}Ti_{0.9}Zr_{0.1}O_3$ceramic sample.

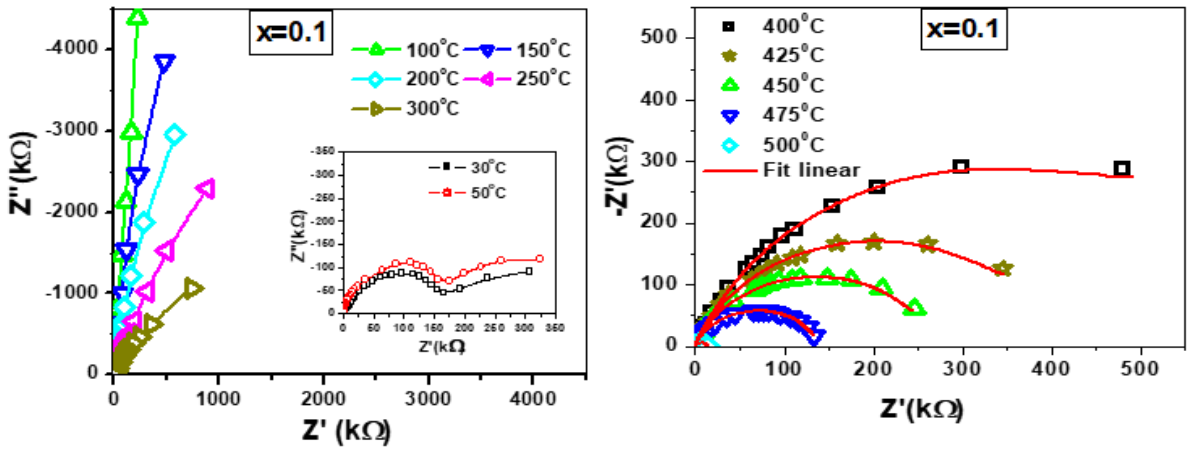

Fig. 9. Variation of Z' with Z'' at different temperature of $Na_{0.5}Bi_{0.5}Ti_{0.9}Zr_{0.1}O_3$.

International Journal of Engineering Research & Technology (IJERT)
ISSN: 2278-0181
Vol. 9 Issue 01, January-2020

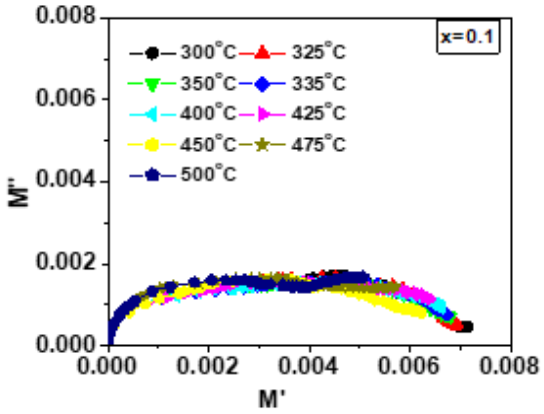

Fig. 10. Variation of M' with M'' at different temperature of $Na_{0.5}Bi_{0.5}Ti_{0.9}Zr_{0.1}O_3$.

3.5 Polarisation study

The hysteresis loop of the samples poled at a field of 6-6.5 kV/cm for 24 h in silicon oil bath is obtained using precision workstation (P~E loop tracer, Marine India, New Delhi). Figure 11 represents the room temperature hysteresis loop of **$Na_{0.5}Bi_{0.5}Ti_{0.9}Zr_{0.1}O_3$** compound. As dielectric breakdown of the prepared ferroelectric samples occurs at a lower field, as a result, the saturation polarization could not be obtained at the experimental range of field. Therefore, we are unable to obtain a proper P~E loop. Using the hysteresis loop tracer, polarization of the prepared samples of different thickness and area are measured. The anomaly obtained in dielectric plots of the prepared compounds as observed in previous section is correlated with ferro to para phase transition, which is confirmed from the nature of P~E loop obtained.

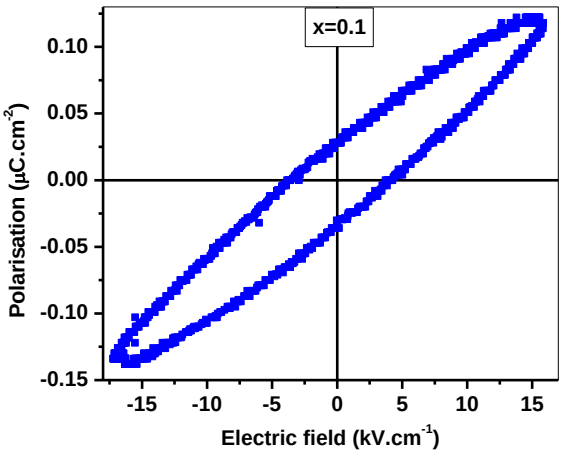

Fig. 11 P~E loop of $Na_{0.5}Bi_{0.5}Ti_{0.9}Zr_{0.1}O_3$ at room temperature.

High-leakage current and partial reversal polarization causes the unsaturated hysteresis loops noticed for all the samples under the applied field. The low value of polarization is because of lesser size of bulk size which results a plenty of bulk interfaces. The bulk interfaces are the regime where permittivity is very low and it causes poor ferroelectricity in the materials. The polarization becomes discontinuous at the interface and surface of bulk, which results a decrease in polarization ($2P_r$) [28].

4. CONCLUSION

The polycrystalline sample of NBTZ was set up by a solid state-reaction course. Fundamental X-ray assessment asserts the single stage orthorhombic crystal structure at room temperature. The plot positively settled the ferro to paraelectric stage change at 268˚C. Addition of Zr builds room temperature and peak dielectric constant values, which can be valuable for dielectric for capacitor application. The dielectric constant of the ceramics lessens with expanding frequency. Impedance and modulus spectroscopy uncovers the nearness of grain and grain boundary commitment in the sample. The activation energy of the compound was seen as particular in different regions showing nearness of different conduction segments.

ACKNOWLEDGEMENTS

D. Panda recognizes North Orissa University for the co-activity and help during his Ph.D research work. He very appreciative to Director, PXE, Chandipur, for permitting him for the exploration program.The authors are grateful to Prof. R.N.P. Choudhary, Professor, Department of Physics, ITER, Bhubaneswar who had helped us and allowed us to

International Journal of Engineering Research & Technology (IJERT)
ISSN: 2278-0181
Vol. 9 Issue 01, January-2020

utilize his laboratary during synthesis of compound and some of investigation of its properties. D. Panda additionally recognizes Department of Physics, Betnoti College Betnoti for enabling him to do some trial work during his examination.

CONFLICTS OF INTEREST

The authors pronounce no irreconcilable situations with respect to the publication of this paper.

REFERENCES

[1] Mahajan S, Thakur O P and Prakash C 2009 *J. Alloy Compds***471** 507
[2] Mahajan S, Thakur O P, Bhattacharya D K and Sreenivas K 2008 *Mater. Chem. Phys.* **112** 858
[3] Mahajan S, Thakur O P, Bhattacharya D K and Sreenivas K 2009 *J. Am. Ceram.. Soc.* **92** 416
[4] Maiti T, Guo R and Bhalla A S 2006a *Appl. Phys. Lett.* **100** 114109
[5] Maiti T, Guo R and Bhalla A S 2006b *Appl. Phys. Lett.* **89** 122909
[6] Zhu, X.L., Chen, X.M., Liu, X.Q. and Yuan, Y. (2006) Dielectric Characteristics and Diffuse Ferroelectric Phase Transition in Sr4La2Ti4Nb6O30 Tungsten Bronze Ceramics. Journal of Materials Research, 21, 1787-1792. https://doi.org/10.1557/jmr.2006.0201
[7] Huang, C., Bhalla, A.S. and Guo, R. (2005) Measurement of Microwave Electro-Optic Coefficient in Sr0.61Ba0.39Nb2O6 Crystal Fiber. Applied Physics Letters ,86, Article ID: 211907. https://doi.org/10.1063/1.1937997
[8] Ramirez, M.O., Jaque, D., Bausa, L.E., Sole Garci, J. and Kaminskii, A.A. (2005) Near Infraredand Visible Tunability from a Diode Pumped Nd Activated StrontiumBarium Niobate Laser Crystal. Physical Review Letters , 95, Article ID: 267401.
[9] Rao, K.S. and Nath, N.V. (2005) Influence of Rare-Earth Ion on Piezoelectric and Pyroelectric Properties of PBN System. Ferroelectrics, 325, 15-24. https://doi.org/10.1080/00150190500326605
[10] Jiang, W., Cao, W., Yi, X. and Chen, H. (2005) The Elastic and Piezoelectric Properties of Tungsten Bronze Ferroelectric Crystals (Sr0.7Ba0.3)2NaNb5O15 and (Sr0.3Ba0.7)2NaNb5O15. Journal of Applied Physics , 97, Article ID: 094106. https://doi.org/10.1063/1.1881777
[11] Raju, M.R. and Choudhary, R.N.P. (2006) Effect of Zr Substitution on Structural, Dielectric and Electrical Properties of Sr5SmTi3Nb7O30 Ceramics. Materials Chemistry and Physics, 99, 135-143. https://doi.org/10.1016/j.matchemphys.2005.09.084
[12] Chen, W., Kinemuchi, Y., Watari, K., Tamura, T. and Miwa, K. (2006) Preparation of Grain-Oriented Sr0.5Ba0.5Nb2O6 Ferroelectric Ceramics by Magnetic Alignment. Journal of the American Ceramic Society , 89, 381-384. https://doi.org/10.1111/j.1551-2916.2005.00694.x
[13] Ko, H., Kojima, S., Lushnikov, S.G., Katiyar, R.S., Kim, T.-H. and Ro, J.-H. (2002) Low-Temperature Transverse Dielectric and Pyroelectric Anomalies of Uniaxial Tungsten Bronze Crystals. Journal of Applied Physics , 92, 1536. https://doi.org/10.1063/1.1491995
[14] Wu, E. (1989) POWD, an Interactive Powder Diffraction Data Interpretation and Index Program. Ver.2.1. School of Physical Science, Flinders University South Bedford Park, Australia.
[15] Geiss, E.A., Scott, B.A., Burns, G., O'Kane, D.F. and Segmuller, A. (1969) Alkali Strontium-Barium-Lead Niobate Systems with a Tungsten Bronze Structure: Crystallographic Properties and Curie Points. Journal of the American Ceramic Society ,52, 276-281. https://doi.org/10.1111/j.1151-2916.1969.tb09183.x
[16] Klug, H.P. and Alexander, L.E. (1974) X-Ray Diffraction Procedures for Polycrystalline and Amorphous Materials. Willey-Interscience, New York.
[17] Sahho, P.S., Panigrahi, A., Patri, S.K. and Choudhary, R.N.P. (2010) Impedanc Spectroscopy of Ba3Sr2DyTi3V7O30 Ceramic. Bulletin of Materials Science , 33,129-134. https://doi.org/10.1007/s12034-010-0018-8
[18] Dash, S., Choudhary, R.N.P. and Kumar, A. (2014) Impedance Spectroscopy and Conduction Mechanism of Multiferroic (Bi0.6K0.4)(Fe0.6Nb0.4)O3. Journal of Physics and Chemistry of Solids , 75, 1376-1382. https://doi.org/10.1016/j.jpcs.2014.07.018
[19] Singh, A.K., Barik, S.K., Choudhary, R.N.P. and Mahapatra, P.K. (2009) Ac Conductivity and Relaxation Mechanism in Ba0.9Sr0.1TiO3. Journal of Alloys and Compounds, 479, 39-42. https://doi.org/10.1016/j.jallcom.2008.12.130
[20] Bhattacharya, S., Bharadwaj, S.S.N. and Krupanidhi, S.B. (2000) Alternating Current Conduction Behavior of Excimer Laser Ablated SrBi2Nb2O9 Thin Films. Journal of Applied Physics , 88, 4294. https://doi.org/10.1063/1.1287782
[21] P.S.Sahoo, A. Panigrahi, S.K. Patri, R.N.P. Choudhary, *Bull.Metr.Sc.* **33 (2)** (2010) 129.
[22] S. Saha, T.P. Sinha, Phys. Rev. B **65** (2002)134103.
[23] S. Sen, P. P.ramanik, R.N.P Choudhary, Appl. Phys. A**82**(2006) 549
[24] Y. Hosono, K. Harada, Y.Yamashita, Jpn. J.Appl.Phys. **40** (2001)5722.
[25] D.C. Sinclair, A.R. West, "Impedance and modulus spectroscopy of semiconducting BaTiO3 showing positive temperature coefficient of resistance", J. Appl. Phys., 66 (1989) 3850.
[26] S. Sahoo, P.K. Mahapatra, R.N.P. Choudhary, "The structural, electrical and magnetoelectric properties of softchemically-synthesized SmFeO3 ceramics", J. Phys. D:Appl. Phys., 49 (2016) 035302.
[27] S.K. Dehury, K. Parida, R.N.P. Choudhary, "Dielectric,impedance and magneto-electric characteristics of Bi0.5Sr0.5Fe0.5Ce0.5O3 electronic material", J. Mater. Sci.:Mater. Electron., 28 (2017) 10441–10448.
[28] B. Garbarz-Glos, W. B, ak, M. Antonova, M. Pawlik,"Structural, microstructural and impedance spectroscopy study of functional ferroelectric ceramic materials based on barium titanate", IOP Conf. Ser.: Mater. Sci. Eng., 49 (2013) 012031.
[29] B.E. Vugmeister, M.D. Glinichuk, "Dipole glass and ferroelectricity in random-site electric dipole systems", Rev.Mod. Phys., 62 (1990) 993–1026.
[30] R. Ranjan, R. Kumar, N. Kumar, B. Behera, R.N.P.Choudhary, "Impedance and electric modulus analysis of Sm-modified Pb(Zr0.55Ti0.45)1-x/4O3 ceramics", J. Alloys Compd., 509 (2011) 6388–6394.
[31] A. Rouahi, A. Kahouli, F. Challali, M.P. Besland, C. Vallée, B. Yangui, S. Salimy, A. Goullet, A. Sylvestre, "Impedance and electric modulus study of amorphous TiTaO thin films: Highlight of the interphase effect", J. Phys. D: Appl. Phys., 46 (2013) 065308.
[32] M. Idrees, M. Nadeem, M.M. Hassan, "Investigation of conduction and relaxation in MoS2 nanoflakes synthesized by simple solid state reaction",J. Appl. Phys., 113 [4] (2013) 043704–043706.
[33] Xiao, S.X. and Yan, X.P. (2009) Preparation and Characterization of Si-Doped Barium Titanate Nanopowders and Ceramics.*Microelectronic Engineering*, **86**, 387-391. http://dx.doi.org/10.1016/j.mee.2008.11.042
[34] Rath, M.K., Pradhan, G.K., Pandey, B., Verma, H.C., Roul, B.K. and Anand, S. (2008) Synthesis, Characterization and Dielectric Properties of Europium-Doped Barium Titanate Nanopowders. *Materials Letters*, **62**, 2136-2139. http://dx.doi.org/10.1016/j.matlet.2007.11.033
[35] Gulwade, D. and Gopalan, P. (2008) Diffuse Phase Transition in La and Ga Doped Barium Titanate. *Solid State Communications*, **146**, 340-344. http://dx.doi.org/10.1016/j.ssc.2008.02.018
[36] Unruan, M., Sareein, T., Tangsritrakul, J., Prasetpalichatr, S., Ngamjarurojana, A., Anata, S. and Yimnirun, R. (2008) Changes in Dielectric and Ferroelectric Properties of Fe3+/Nb5+ Hybrid-Doped Barium Titanate Ceramics under Compressive Stress. *Journal of Applied Physics*, **104**, Article ID: 124102. http://dx.doi.org/10.1063/1.3042228
[37] Yaseen, H., Baltianski, S. and Tsur, Y. (2006) Effect of Incorporating Method of Niobium on the Properties of Doped Barium Titanate Ceramics. *Journal of the American Ceramic Society*, **89**, 1584-1589.http://dx.doi.org/10.1111/j.1551-2916.2006.00966.

International Journal of Engineering Research & Technology (IJERT)
ISSN: 2278-0181
Vol. 9 Issue 01, January-2020

[38] Cha, S.H. and Han, Y.H. (2006) Effects of Mn Doping on Dielectric Properties of Mg-Doped BaTiO3. *Journal of Applied Physics*, **100**, Article ID: 104102. http://dx.doi.org/10.1063/1.2386924

[39] Shen, Z.J., Chen, W.P., Qi, J.Q., Wang, Y., Chan, H.L.W., Chen, Y. and Jiang, X.P. (2009) Dielectric Properties of Barium Titanate Ceramics Modified by SiO2 and by BaO-SiO2. *Physica B*: *Condensed Matter*, **404**, 2374-2376.http://dx.doi.org/10.1016/j.physb.2009.04.039

[40] Kirianov, A., Hagiwara, T., Kishi, H. and Ohsato, H. (2002) Effect of Ho/Mg Ratio on Formation of Core-Shell Structure in BaTiO3 and on Dielectric Properties of BaTiO3 Ceramics. *Japanese Journal of Applied Physics*, **41**, 6934-6937. http://dx.doi.org/10.1143/JJAP.41.6934

[41] Wang, S., Zhang, S.R., Zhou, X.H., Li, B. and Chen, Z. (2005) Effect of Sintering Atmospheres on the Microstructure and Dielectric Properties of Yb/Mg Co-Doped BaTiO3 Ceramics. *Materials Letters*, **59**, 2457-2460.http://dx.doi.org/10.1016/j.matlet.2005.03.016

[42] Rout, S.K., Sinha, E. and Panigrahi, S. (2007) Dielectric Properties and Diffuse Phase Transition in Ba1−xMgxTi0.6Zr0.4-O3 Solid Solutions. *Materials Chemistry and Physics*, **101**, 428-432.http://dx.doi.org/10.1016/j.matchemphys.2006.08.002

[43] Henning, D., Schnell, A. and Simon, G. (1982) Diffuse Ferroelectric Phase Transitions in Ba(Ti1-yZry)O3 Ceramics. *Journal of the American Ceramic Society*, **65**, 539-544. http://dx.doi.org/10.1111/j.1151-2916.1982.tb10778.

[44] Yu, Z., Guo, R. and Bhalla, A.S. (2000) Dielectric Behavior of Ba(Ti1−xZrx)O3 Single Crystals. *Journal of Applied Physics*, **88**, 410. http://dx.doi.org/10.1063/1.373674